



# ATLAS B-Physics Results with First Data

---

**Kai Grybel**

*on behalf of the ATLAS collaboration*

*University of Siegen*

*E-mail: grybel@hep.physik.uni-siegen.de*

First data of ATLAS will allow several  $B$ -physics related analyses. Already with  $10 \text{ pb}^{-1}$ , the cross section of heavy quarkonia like  $J/\psi$  and  $\Upsilon$  will be measured in a  $p_T$  range from 10-50 GeV. The  $J/\psi$  and  $\Upsilon$  polarization is expected to be measured with a precision of 0.02 to 0.06 and 0.2 for  $\Upsilon$ , respectively. Another measurement with first data will be the estimation of the cross section of the exclusive decay  $B^+ \rightarrow J/\psi K^+$ , which will be used as a reference channel for e.g. rare  $B$ -decay searches as well as for detector performance studies. For the later the decays  $B_s^0 \rightarrow J/\psi \Phi$  and  $B_d^0 \rightarrow J/\psi K^{0*}$  will be important. The measurement of the invariant masses of  $B$ -mesons and of their lifetimes using these decays will allow to check the detector performance and to study the potential of flavor tagging algorithms, which are crucial for other  $B$ -physics related analyses.

*Flavor Physics and CP Violation 2009*

*May 27 - June 1, 2009*

*Lake Placid, NY, USA*



## 1. Introduction

The ATLAS detector is one of the general purpose experiments of the upcoming LHC (Large Hadron Collider). With a center-of-mass energy of 14 TeV and an instantaneous luminosity of  $\mathcal{L} = 10^{33} \text{cm}^{-2} \text{s}^{-1}$  about  $10^5$   $b\bar{b}/s$  will be produced and will make ATLAS [1] to a  $b$ -factory. Already in the beginning of data-taking ( $\int \mathcal{L} dt \sim 10 \text{ pb}^{-1} - 100 \text{ pb}^{-1}$ )  $B$ -physics analyses and detector performance checks will be performed [1].

An important issue for the analyses as well as detector performance checks will be triggering the events. ATLAS has foreseen a special  $B$ -physics trigger menu, which is explained in section 2.

With an amount of  $\int \mathcal{L} dt \sim 10 \text{ pb}^{-1}$  first measurements of the inclusive and exclusive cross sections will be feasible. Inclusive cross section measurements of prompt heavy quarkonia ( $J/\psi$  and  $\Upsilon$ , see section 3) are being prepared. These measurements will cover a wide  $p_T$  range and will improve measurements of Tevatron [2, 3], which show an excess of prompt quarkonia production compared to predictions of QCD models. Therefore these measurements will contribute to the understanding of the production mechanisms and their phenomenology.

An inclusive cross section measurement of the decay  $B^+ \rightarrow J/\psi K^+$  will be performed (presented in section 4). This decay channel will be used e.g. as a reference in the search for rare  $B$ -decay like  $B_s \rightarrow \mu^+ \mu^-$ .

One possibility for performance checks will be the measurement of the  $B_d^0$  and  $B_s^0$  mass and lifetime using the decays  $B_d \rightarrow J/\psi K^{0*}$  and  $B_s^0 \rightarrow J/\psi \Phi$  (section 5). Also, these decays will be used to calibrate the jet charge tagger.

## 2. B-Physics Trigger

The ATLAS trigger is a three level trigger system. The first level (Lvl 1) trigger consists of different hardware-based trigger, while the second and third level triggers (Lvl 2 and event filter EF) are software-based. Starting from a bunch crossing rate of 40 MHz, the Lvl 1 trigger will reduce the rate to 75 kHz, the Lvl 2 trigger to 2 kHz and finally the EF to a maximum of  $\sim 200$  Hz, which will be written to tape.

The ATLAS trigger menu contains a dedicated  $B$ -physics slice, which triggers on single as well as di-muon events and reconstruct the  $J/\psi$ ,  $\Upsilon$  and  $B$ -masses. About 5 – 10% of the total bandwidth can be used for  $B$ -physics related interests.

### 2.1 Level 1 Trigger

The hardware-based Lvl 1 trigger identifies detector regions, in which the trigger element is found (Regions of Interest, RoI). In the beginning at a instantaneous luminosity of  $10^{31} \text{cm}^{-2} \text{s}^{-1}$  the lowest threshold for single muon triggers will be  $p_T \sim 4 \text{ GeV}$ . This threshold will be increase to  $p_T = 6$  to  $8 \text{ GeV}$  at  $\mathcal{L} = 10^{32} \text{cm}^{-2} \text{s}^{-1}$  for the single muon trigger and  $p_{T1(2)} = 6(4) \text{ GeV}$  for the di-muon trigger. The performance of the different single and di-muon trigger for events containing a promptly produced  $J/\psi$  is shown in fig.1(a).

### 2.2 Level 2 and Event Filter

The Lvl 2 trigger is a software-based trigger. The decision on Lvl 2 is seeded by the RoI of the first trigger level and uses at first information of the muon chambers stand-alone. After that, this

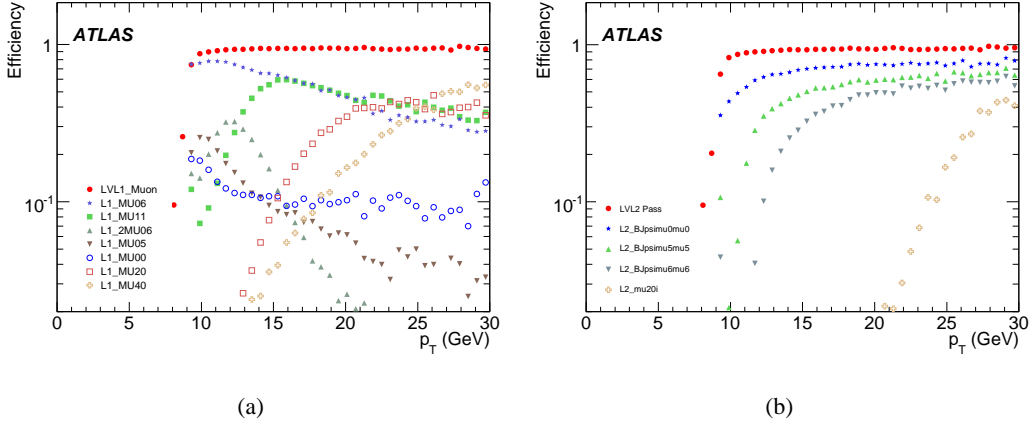


**Figure 1:** Turn-on curves for Lvl 1 (left) and Lvl 2 (right) muon trigger signatures, using events which contains at least one promptly produced  $J/\psi$ .

information is combined with tracking information from the inner detector to reconstruct the track of the muon more precisely and to reject  $\pi$  and  $K$  decays in that way.

In addition the reconstruction of secondary vertices is foreseen on Lvl 2 in order to look for special sub-decays of interest, like  $J/\psi \rightarrow \mu^+\mu^-$ . The performance of the different Lvl 2 triggers with respect to Lvl 1 on prompt  $J/\psi \rightarrow \mu^+\mu^-$  events are shown in fig.1(b).

On EF level, the complete event information is used and adapted offline reconstruction algorithms are available to refine the Lvl 2 decision.

### 3. Physics with Heavy Quarkonium States $J/\psi$ and $\Upsilon$

The heavy quarkonia decays  $J/\psi \rightarrow \mu^+\mu^-$  and  $\Upsilon \rightarrow \mu^+\mu^-$  open up possibilities to check QCD calculations already with an integrated luminosity of  $\int \mathcal{L} dt = 10 \text{ pb}^{-1}$  as well as to perform offline monitoring in order to reveal e.g. problems in detector alignment or non-uniformities of the magnetic field.

#### 3.1 Selection and Reconstruction of Events

Since the heavy quarkonia are producing two muons, a di-muon trigger with  $p_{T(1(2))} > 6(4) \text{ GeV}$  ( $\mu 6\mu 4$ ) is used. In each of the events that passed the trigger, pairs of oppositely charged muon candidates are combined and if the muon system has an invariant mass of  $m_{\mu\mu} > 10 \text{ GeV}$  a common vertex is fitted. The two muons form a quarkonia candidate if the invariant mass of the vertex is  $m_{J/\psi}^{PDG} \pm 300 \text{ MeV}$  and  $m_{\Upsilon}^{PDG} \pm 1 \text{ GeV}$ , respectively.

In order to suppress background contributions which are expected to come mainly from  $b \rightarrow J/\psi + X$  decays and the continuum of di-muon final states from  $b\bar{b}$  events, additional cuts are applied on the pseudo-proper time  $t$ , which is defined as

$$t = \frac{L_{xy} M_{J/\psi}}{p_T(J/\psi)c} \quad (3.1)$$

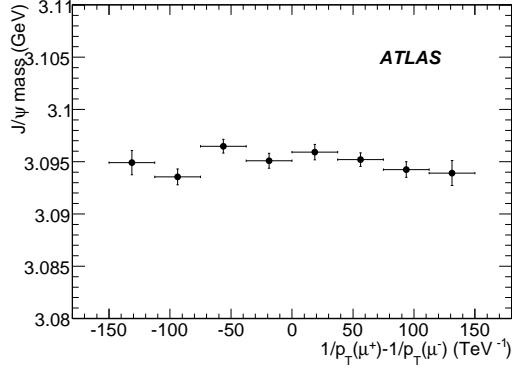


**Figure 2:** Rec. prompt  $J/\psi$  mass as a test for detector horizontal misalignment. Statistics corresponds to  $6 \text{ pb}^{-1}$  of data, no misalignment simulated.

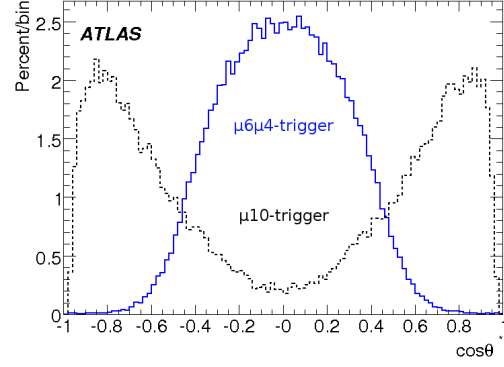


**Figure 3:** Sensitivity of the measurement of  $\cos \theta^*$  for prompt  $J/\psi$  events triggered by a single or di-muon trigger.

where  $L_{xy}$  is transverse decay length distance of the di-muon vertex,  $p_T(J/\psi)$  the transverse momentum and  $M_{J/\psi}$  the mass of the  $J/\psi$  candidate. In tab.1 the reconstruction efficiencies and the signal to background ratios are shown.

Quarkonium	prompt $J/\psi$	prompt $\Upsilon$
$\varepsilon$ [%]	67	49
Signal/Backgr. at peak	60	10

**Table 1:** Reconstruction efficiencies and signal to background ratio for prompt  $J/\psi$  and  $\Upsilon$  events.

### 3.2 Offline Monitoring using Quarkonia

Possible systematic shifts of the reconstructed mass of the  $J/\psi$  vs.  $p_T$  reveal problems with the  $\mu$ -momentum scale or with the energy loss corrections. In case of unknown material effects or magnetic field non-uniformities shifts of the mass vs.  $\eta$  would occur. Horizontal misalignment of detector parts would cause a shift in the mass distribution as a function of the curvature difference of the two muon tracks (see fig.2, for a dataset where no misalignment was simulated).

Due to the mass of the  $J/\psi$  and  $\Upsilon$  being lower than the mass of e.g. the  $Z$ -boson, these checks are complementary to the checks which can be done e.g. with  $Z$ -boson samples.

### 3.3 Measurement of Polarisation and Cross Section

Theory models like the Color-Singlet (CSM) [4] or Color-Octet model (COM) [5] aim at reproducing production properties of heavy quarkonia. While the rate of produced heavy quarkonia cannot be explained by the CSM but in the COM, the COM fails by reproducing the polarization of the produced particles. Therefore measurements of the cross section and the polarization will help to understand the production mechanisms.

The polarisation parameter  $\alpha = (\sigma_T - 2\sigma_L)/(\sigma_T + 2\sigma_L)$  is extracted by measuring

$$\frac{dN}{d\cos\theta^*} = C \frac{3}{2\alpha + d} (1 + \alpha \cos^2\theta^*) \quad (3.2)$$

where  $\theta^*$  is defined as the angle between the positively charged muon from the quarkonium decay in the restframe of the quarkonium and the flight direction of the quarkonium in the laboratory frame. Small values of  $\cos \theta^*$  corresponds to events where both muons have similar  $p_T$  while  $\cos \theta^* \sim 1$  leads to events with one high  $p_T$  muon. Therefore the kinematical acceptance on  $\cos \theta^*$  for events selected by a di-muon trigger is complementary to a single-muon trigger (e.g.  $p_T > 10, \mu 10$ ) based selection (see fig.3). An improvement for the measurement can be achieved by combining both sample.

Taking into account both trigger signatures, the polarisation is expected to be measured at  $10 \text{ pb}^{-1}$  with a precision of 0.02 to 0.06 for  $J/\psi$  and  $\sim 0.2$  for  $\Upsilon$ . The cross section precision is expected to be about 1% (5%) for prompt  $J/\psi$  ( $\Upsilon$ ) in a  $p_T$  range of 10 – 50 GeV, which can be increased to about 100 GeV once more than  $100 \text{ pb}^{-1}$  of data will be available.

#### 4. Cross Section Measurement with $B^+ \rightarrow J/\psi K^+$

The inclusive cross section measurement in the  $B^+ \rightarrow J/\psi(\mu^+\mu^-)K^+$  channel will be started with already  $10 \text{ pb}^{-1}$ . It will reduce uncertainties in the overall  $b\bar{b}$  cross section estimation, which currently can only be extrapolated from Tevatron to LHC energies with an uncertainty factor of about two. In addition, this decay will be the reference channel for other analyses like searches for rare  $B$ -decays.

##### 4.1 Selection and Reconstruction of Events

The reconstruction is started by looking for  $J/\psi \rightarrow \mu^+\mu^-$ . Two oppositely charged muon candidates ( $p_{T\mu 1} > 6 \text{ GeV}$ ,  $p_{T\mu 2} > 3 \text{ GeV}$ ) are fitted to a common vertex. The tracks form a  $J/\psi$  candidate if the proper decay length  $\lambda < 0.1 \text{ mm}$ , in order to reduce background from prompt  $J/\psi$ . The invariant mass window is chosen to be  $m_{J/\psi}^{PDG} \pm 120 \text{ MeV}$ .

The  $J/\psi$  candidate will be combined with a positively charged track ( $p_T > 1.5 \text{ GeV}$ ,  $|\eta| < 2.5$ ), which is inconsistent with coming from the primary vertex ( $|d_0|/\sigma_{d_0} > 1$ ), to a common secondary vertex. The reconstructed momentum of the  $B^+$  candidate has to point to the primary vertex to be retained.

##### 4.2 $B^+$ Mass Determination

A maximum likelihood fit to the invariant mass spectrum of the  $B^+$  candidate is done in order to fit the  $B^+$  mass distribution. The likelihood uses a Gaussian distribution for the signal and a linear function for background. For an integrated luminosity of  $10 \text{ pb}^{-1}$  the  $B^+$ -mass resolution is estimated to  $\sigma = 42.2 \pm 1.3 \text{ MeV}$ .

##### 4.3 Measurement of the Cross Section

The differential cross section is obtained from

$$\frac{d\sigma(B^+)}{dp_T} = \frac{N_{sig}}{\mathcal{L} \epsilon \Delta p_T BR(B^+ \rightarrow J/\psi K^+)} \quad (4.1)$$

where the number of signal events  $N_{sig}$  as well as the efficiency  $\varepsilon$  can be determined from the likelihood fit (see section 4.2) done for different  $p_T$  bins. The total efficiency is estimated to  $29.8 \pm 0.8\%$ .

The statistical error of this measurement using  $10 \text{ pb}^{-1}$  of data is expected to be smaller than 5% for the total and smaller than 10% for the differential cross section measurement. Tab.2 summarizes the expected statistical (inclusive the error on the efficiency) and total uncertainties for different  $p_T$  bins as well as for the total cross section measurement. The main sources of systematic uncertainties are the integrated luminosity, which is expected to be known to a precision of 10% in the beginning, and the error on the branching fraction of 10%. The statistical uncertainty will decrease to percent level once  $\geq 100 \text{ pb}^{-1}$  of data is available, while the error on the luminosity is expected to be approximately 6.5% at  $\geq 300 \text{ pb}^{-1}$  will be available.

$p_T$ -range	$p_T \in [10, 18]$	$p_T \in [18, 26]$	$p_T \in [26, 34]$	$p_T \in [34, 42]$	$p_T \in [10, \infty]$
Statistical + $\varepsilon$ [%]	7.7	6.9	10.5	13.9	4.3
total [%]	16.1	15.8	17.6	19.8	14.8

**Table 2:** Statistical and total uncertainties of the cross section measurement for different  $p_T$  bins.

## 5. Performance Measurements with $B_s^0 \rightarrow J/\psi\Phi$ and $B_d^0 \rightarrow J/\psi K^{0*}$

The decay channels  $B_s^0 \rightarrow J/\psi(\mu^+\mu^-)\Phi(K^+K^-)$  and  $B_d^0 \rightarrow J/\psi(\mu^+\mu^-)K^{0*}(K^\pm\pi^\mp)$  are expected to yield high event statistics. Therefore physics and detector performance checks are possible with already  $10 - 150 \text{ pb}^{-1}$  by measuring the mass and the lifetime of the  $B$ -hadron.

Later on with an integrated luminosity of about  $150 \text{ pb}^{-1}$  it will be possible to start calibrating more sophisticated algorithms like the jet charge tagger, which allows to distinguish the flavour of a  $B$ -meson. This will be important for CP-violation and  $B_s$ -oscillation analyses.

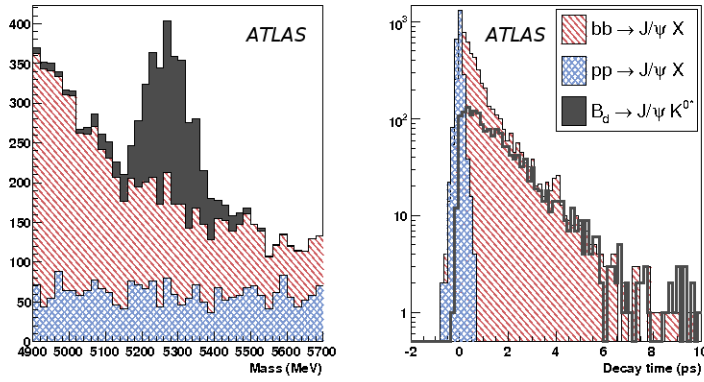
### 5.1 Selection and Reconstruction of Events

The reconstruction of exclusive  $B_d^0$  and  $B_s^0$  decays starts with the reconstruction of the  $J/\psi \rightarrow \mu^+\mu^-$  sub-decay. Oppositely charged muons with  $p_{T\mu_1} > 6 \text{ GeV}$ ,  $p_{T\mu_2} > 4 \text{ GeV}$  and  $|\eta_{\mu_{1/2}}| < 2.4$  are fitted to a common vertex. The two muons form a  $J/\psi$  candidate if the invariant mass lies inside a mass window of  $3\sigma$  ( $\sigma = 58 \text{ MeV}$ ) around the nominal  $J/\psi$  mass.

The  $\Phi \rightarrow K^+K^-$  ( $K^{0*} \rightarrow K^\pm\pi^\mp$ ) sub-decay is reconstructed by combining two oppositely charged tracks, which are not identified as muons, with  $p_T > 0.5 \text{ GeV}$  and  $|\eta| < 2.5$  to a common vertex. After a cut on the invariant mass, this track pair forms a  $\Phi$  ( $K^{0*}$ ) candidate.

To reconstruct the  $B_s^0$  ( $B_d^0$ ) the  $J/\psi$  and the  $\Phi$  ( $K^{0*}$ ) candidate are fitted to a common vertex, which has to have  $p_T > 10 \text{ GeV}$ . The  $B_{d/s}^0$  candidate is accepted if the invariant mass is in a region of  $\pm 12\sigma$  of the  $B$ -hadron mass. In order to reduce background contributions from e.g. prompt  $pp \rightarrow J/\psi X$  but also from  $b\bar{b} \rightarrow J/\psi X$ , a cut on the  $B$ -decay time  $t > 0.5 \text{ ps}$  can be applied once the vertexing and the alignment of the inner detector are well understood. Tab.3 presents the efficiency of reconstruction for signal and background events with and without a cut on the  $B$ -decay time.

	Efficiency [%]	
	before time cut	after time cut
Signal $B_d^0 \rightarrow J/\psi K^{0*}$	42.0	30.4
$pp \rightarrow J/\psi X$ (bck. 1)	0.67	0.0064
$b\bar{b} \rightarrow J/\psi X$ (bck. 2)	3.05	1.52
Signal $B_s^0 \rightarrow J/\psi \Phi$	40.5	30.0
$pp \rightarrow J/\psi X$ (bck. 1)	1.5	0.0058
$b\bar{b} \rightarrow J/\psi X$ (bck. 2)	1.1	0.8

**Table 3:** Efficiencies to reconstruct signal and a background events.**Figure 4:** Distributions of reconstructed lifetime for the  $B_d^0 \rightarrow J/\psi K^{0*}$  and background contributions.

## 5.2 Estimation of Mass and Lifetime

In order to estimate the mass and the lifetime of  $B$ -hadron a simultaneous maximum likelihood fit is done. The distributions for the mass and the decay time for the  $B_d^0 \rightarrow J/\psi K^{0*}$  signal and the various backgrounds is shown in fig.4.

The fit results and their statistical errors are shown in tab.4. With  $10 \text{ pb}^{-1}$  the lifetime is expected to be measured with an relative uncertainty of  $\sim 10\%$  and a resolution of  $\sim 0.1 \text{ ps}$ . The mass resolution is expected to be in the order of  $50 - 60 \text{ MeV}$ .

Parameter	Fit results with stat. error	
	$B_d^0$ ( $10 \text{ pb}^{-1}$ )	$B_s^0$ ( $150 \text{ pb}^{-1}$ )
$\Gamma$ [ $\text{ps}^{-1}$ ]	$0.73 \pm 0.07$	$0.743 \pm 0.051$
$m(B)$ [GeV]	$5.284 \pm 0.006$	$5.359 \pm 0.006$
$\sigma$ [ps]	$0.132 \pm 0.004$	$0.152 \pm 0.001$
$\sigma_m$ [GeV]	$0.054 \pm 0.006$	$0.061 \pm 0.006$

**Table 4:** Mass and lifetime fit results for  $B_d^0$  and  $B_s^0$  corresponding to a integrated luminosity of  $10 \text{ pb}^{-1}$  and  $150 \text{ pb}^{-1}$ , respectively. Errors are statistical only.

### 5.3 Calibration of the Jet Charge Tagger

Most of the CP violation studies require  $B$ -meson flavour tagging. This may be achieved with the jet charge tagger in a statistical way. All tracks in a cone with an opening angle  $\Delta R^1$  around a  $B$ -meson are taken into account in order to calculate the jet charge  $Q_{jet}$

$$Q_{jet} = \frac{\sum_i q_i p_{L_i}^\kappa}{\sum_i |p_{L_i}|^\kappa} \quad (5.1)$$

where  $q_i$  is the charge of the  $i^{th}$  track and  $p_{L_i}$  is the projection of the momentum along the flight direction of the  $B$ -meson. The exponent  $\kappa$  is a free parameter to tune the tagger. Additional parameters are the minimal allowed  $|Q_{jet}|$  (*exclusion cut*) as well as the opening angle of the cone  $\Delta R$  around the  $B$ -meson. Due to the fragmentation of the  $b$ -quarks,  $b$ -quark induced jets tend to have a jet charge  $Q_{jet} < 0$  and  $\bar{b}$ -quark induced jets to  $Q_{jet} > 0$ , respectively.

The performance of the jet charge tagger can be estimated by defining the efficiency  $\varepsilon$  and the wrong tag fraction  $w_{tag}$  or alternatively the dilution  $D_{tag}$ :

$$\varepsilon = \frac{N_r + N_w}{N_t} \quad (5.2)$$

$$D_{tag} = \frac{N_r - N_w}{N_r + N_w} = 1 - 2w_{tag} \quad (5.3)$$

where  $N_r$  is the number of correctly and  $N_w$  the number of incorrectly identified  $B$  or  $\bar{B}$  mesons out of the  $N_t$  reconstructed  $B$ -mesons.

In the exclusively reconstructed decay channel  $B_d^0 \rightarrow J/\psi K^{0*}$  with a further decay of the  $K^{0*}$  to charged mesons, the initial flavour of the  $B$ -meson is determined in a statistical way. Therefore, this decay channel is considered as self-calibrating w.r.t. the jet charge tagger and will be used to calibrate and to test the performance of the jet charge tagger. For tests and the calibration of the jet charge tagger using the decay channel  $B_s^0 \rightarrow J/\psi \Phi$  more integrated luminosity by a factor of  $\sim 10$  is needed due to a lower cross section compared to the  $B_d^0$  channel. First results can be expected with  $\int \mathcal{L} dt = 1.5 \text{ fb}^{-1}$ .

Tab.5 presents results for the expected performance of the jet charge tagger after optimizing the free parameter for each of the two different decays.

Parameter	$B_d^0$ (150 pb $^{-1}$ )	$B_s^0$ (1.5 fb $^{-1}$ )
Efficiency $\varepsilon$	$0.870 \pm 0.003$	$0.625 \pm 0.005$
Wrong tag fraction $w_{tag}$	$0.380 \pm 0.004$	$0.374 \pm 0.005$
$\varepsilon D_{tag}^2$	$0.050 \pm 0.004$	$0.039 \pm 0.003$

**Table 5:** Performance of the jet charge tagger for the  $B_d^0$  and the  $B_s^0$  decay channels.

## 6. Summary and Conclusions

The  $B$ -physics program with first data of ATLAS provides important input for detector performance tests and detector calibration as well as first physics measurements.

---

<sup>1</sup>  $\Delta R$  is defined as  $\Delta R = \sqrt{\Delta\phi^2 + \Delta\eta^2}$



Already with  $10 \text{ pb}^{-1}$  of data the inclusive cross section of heavy quarkonia, i.e. prompt produced  $J/\psi$  and  $\Upsilon$  can be determined with a precision of  $\sim 1\%$  and  $\sim 5\%$  respectively, which will help to understand the production mechanisms of prompt heavy quarkonia. Furthermore, the polarization of the quarkonia is expected to be measured with a precision of 0.02 to 0.06 for  $J/\psi$  and  $\sim 0.2$  for  $\Upsilon$ , respectively.

An exclusive cross section measurement of  $B^+ \rightarrow J/\psi K^+$  will provide a measurement of the differential cross section as a function of  $p_T$  with uncertainties of 15 – 20% and a total cross section measurement with errors in the order of 15%.

Furthermore, the mass of  $B_d^0$  can be measured to an accuracy of 0.02% and the mass resolution is expected to be  $\sigma(m_{B_d^0}) = 54 \pm 6 \text{ MeV}$ .

With higher statistics of about  $150 \text{ pb}^{-1}$  the decay channel  $B_s^0 \rightarrow J/\psi \Phi$  can be used. The mass of  $B_s^0$  can be determined to an accuracy of 0.02% and a mass resolution of  $\sigma(m_{B_s^0}) = 61 \pm 6 \text{ MeV}$  is expected. The uncertainty of the exclusive cross section measurement is expected to be in the order of 1%.

Within this amount of data the jet charge tagger can be calibrated and tested using decay channels like  $B_d^0 \rightarrow J/\psi K^{0*}$ . Calibrations of the jet charge tagger with  $B_s^0 \rightarrow J/\psi \Phi$ , more statistics by a factor of  $\sim 10$  will be needed.

## Acknowledgements

The author would like to thank the ATLAS B-physics group, especially S. Hassani, C. Petridou, W. Walkowiak, V. Kartvelishvili and M. Smizanska. He also thanks the conference team for organizing the FPCP2009 conference and is grateful to the German Ministry for Education and Research (BMBF) for financial support.

## References

- [1] Aad. G. et al. [ATLAS Collaboration], CERN-OPEN-2008-020 (2008)
- [2] Abazov, V.M. et al. [D0 note], DØ Note 5089-conf (2007)
- [3] Abe, F. et al. [CDF Collaboration], Phys. Rev. Letters 69 (1992) 3704
- [4] See e.g. V.G. Kartvelishvili, A.K. Likhoded, S. R. Slabospitsky, Sov. J. Nucl. Phys. 28 (1978) 280; M. Gluck, J. F. Owens and E. Reya, Phys. Rev. D17 (1978) 2324; E. L. Berger and D. L. Jones, Phys. Rev. D23 (1981) 1521; V. G. Kartvelishvili, A. K. Likhoded, Sov. J. Nucl. Phys. 39 (1984) 298; B. Humpert, Phys. Lett. B184 (1987) 105
- [5] G. T. Bodwin, E. Braaten and G. P. Lepage, Phys. Rev. D51 (1995) 1125 [Erratum-ibid. D55 (1997) 5853] [arXiv:hep-ph/9407339]; E. Braaten and S. Fleming, Phys. Rev. Lett. 74 (1995) 3327 [arXiv:hep-ph/9411365]